Journal of Materials Chemistry

Cite this: J. Mater. Chem., 2011, 21, 17855

www.rsc.org/materials

PAPER

Tailoring balance of carrier mobilities in solid-state light-emitting electrochemical cells by doping a carrier trapper to enhance device efficiencies

Chih-Teng Liao,[a] Hsiao-Fan Chen,[b] Hai-Ching Su*[a] and Ken-Tsung Wong*[b]

Received 12th July 2011, Accepted 5th September 2011
DOI: 10.1039/c1jm13245h

We demonstrate the improving balance of carrier mobilities in neat-film light-emitting electrochemical cells (LECs) utilizing a cationic transition metal complex (CTMC) as the emissive material and a cationic near-infrared laser dye as the carrier trapper. This low-gap carrier trapper is judiciously chosen such that a significant energy offset in the highest occupied molecular orbital (HOMO) levels between the CTMC and the carrier trapper impedes hole transport in the emissive layers while similar lowest unoccupied molecular orbital (LUMO) levels of these two materials result in relatively unaffected electron transport. Since the CTMC neat films would intrinsically exhibit characteristics of preferred transport of holes, the balance of carrier mobilities would be improved by doping such carrier trapper. Electroluminescent measurements show that the peak external quantum efficiency (EQE) and the peak power efficiency of the neat-film LECs doped with the carrier trapper reach 12.75% and 28.70 lm W^{-1}, respectively. These device efficiencies represent a 1.4 times enhancement as compared to those of the undoped neat-film LECs and approach the upper limit of EQE (~15%) that one would expect from the photoluminescence quantum yield of the emissive layer (~0.75) and an optical out-coupling efficiency of ~20% from a typical layered device structure, consequently indicating superior balance of carrier mobilities in such a doped emissive layer. These results confirm that the balance of carrier mobilities in the CTMC neat films would be improved by doping a proper carrier trapper and this technique offers a general approach for optimizing device efficiencies of CTMC-based neat-film LECs.

Introduction

Solid-state light-emitting electrochemical cells (LECs) possess several advantages over conventional organic light emitting diodes (OLEDs). In LECs, electrochemically doped regions induced by spatially separated ions under a bias form ohmic contacts with electrodes, giving balanced carrier injection, low operating voltages, and consequently high power efficiencies.[1,2] As such, LECs generally require only a single emissive layer, which can be easily processed from solutions,[3–5] and can conveniently use air-stable electrodes, while OLEDs typically require more sophisticated multilayer structures and low-work-function cathodes.[6–10] Compared with conventional polymer LECs that are usually composed of an emissive conjugated polymer, a salt and an ion-conducting polymer,[1,2] LECs based on cationic transition metal complexes (CTMCs) show several further advantages and have attracted much attention in recent years.[11–60] In such devices, no ion-conducting material is needed since these CTMCs are intrinsically ionic. Furthermore, higher electroluminescent (EL) efficiencies are expected due to the phosphorescent nature of CTMCs.

In general, CTMC-based LECs are composed of neat films of emissive materials.[11–60] Since the electrochemically doped regions form ohmic contacts with electrodes, the carrier injection at both electrodes is balanced and the carrier recombination zone may consequently locate near one of the electrodes due to a discrepancy in electron and hole mobilities of the emissive layer. The recombination zone in the vicinity of an electrode may cause exciton quenching such that the device efficiency would decrease.[61] Balanced electron and hole mobilities would be beneficial in keeping the recombination zone near the center of the emissive layer and thus would prevent exciton quenching. However, only a few reports successfully demonstrated perfect external quantum efficiencies (EQEs) of CTMC-based LECs reaching the upper limits estimated from the photoluminescence quantum yields (PLQYs) of the emissive layers and an optical out-coupling efficiency of ~20% from a typical layered light-emitting device structure.[33,36,44] Most reported LECs commonly suffered deteriorated device efficiencies due to the intrinsically imperfect balance of carrier mobilities in the neat-film emissive

[a]*Institute of Lighting and Energy Photonics, National Chiao Tung University, Tainan, 71150, Taiwan. E-mail: haichingsu@mail.nctu.edu.tw; Fax: +886-6-3032535; Tel: +886-6-3032121-57792*
[b]*Department of Chemistry, National Taiwan University, Taipei, 10617, Taiwan. E-mail: kenwong@ntu.edu.tw; Fax: +886-2-33661667; Tel: +886-2-33661665*

layers. Hence, to generally optimize the device efficiencies of neat-film LECs based on CTMCs, tailoring the balance of carrier mobilities in the emissive layer to keep the carrier recombination zone away from electrodes would be a critical issue.

Sophisticated design of carrier transporting substituents on CTMCs or introducing proper carrier trappers into the neat-film CTMC emissive layers would be two possible ways to alter carrier mobilities and thus to improve the balance of carrier mobilities. The former method could be implemented by modifying ligands of efficient CTMCs with substituents containing electron and hole transporting moieties.[58] However, adjusting carrier transporting characteristics of CTMCs by modifying their ligands would simultaneously alter their energy gaps and PLQYs, influencing the EL spectra and device efficiencies of LECs.[58] It could not be a general technique for applying to all reported efficient CTMCs. On the other hand, introducing carrier trappers into neat-film CTMC emissive layers could impede carrier transport due to the energy offset in the highest occupied molecular orbital (HOMO) levels or in the lowest unoccupied molecular orbital (LUMO) levels between the CTMCs and the carrier trappers. Different amounts of energy offset in the HOMO levels and in the LUMO levels between the CTMCs and the carrier trappers lead to different degrees of impeding in hole and electron transport, respectively. Therefore, the balance of carrier mobilities in CTMC-based neat-film LECs could be generally optimized by introducing carrier trappers possessing proper HOMO and LUMO levels into the emissive layers.

In this work, we demonstrate improvements in the balance of carrier mobilities in neat-film LECs utilizing a cyan-emitting phosphorescent CTMC as the emissive material and a cationic fluorescent near-infrared (NIR) laser dye as the carrier trapper. This low-gap carrier trapper is chosen such that a significant energy offset in the HOMO levels between the CTMC and the carrier trapper impedes hole transport in the emissive layers while similar LUMO levels of these two materials result in relatively unaffected electron transport. Therefore, the balance of carrier mobilities of the neutral light-emitting layer between the p- and n-type electrochemically doped layers[60] in CTMC neat films, which would intrinsically exhibit characteristics of preferred transport of holes, would be improved by doping such a carrier trapper. Photoluminescence (PL) measurements reveal inefficient energy transfer between the CTMC and the carrier trapper due to poor spectral overlap between the CTMC emission and the carrier-trapper absorption, ensuring unapparent carrier-trapper emission and thus reducing color shift in the CTMC emission at low doping concentrations of the carrier trapper. However, even at low doping concentrations, carrier trapping would still be effective due to the large energy offset in the HOMO levels between the CTMC and the carrier trapper. EL measurements show that the peak EQE (power efficiency) of the neat-film LECs doped with the carrier trapper reaches 12.75% (28.70 lm W^{-1}), representing a 1.4 times enhancement in device efficiency as compared to that of the undoped neat-film LECs. Such device efficiency approaches the upper limit (~15%) that one would expect from the PLQY of the emissive layer (~0.75) and an optical outcoupling efficiency of ~20% from a typical layered light-emitting device structure, consequently indicating superior balance of carrier mobilities in such doped emissive layer. These results confirm the strategy of introducing a proper carrier trapper into the CTMC neat films would improve the balance of carrier mobilities in the emissive layer, offering a general approach for optimizing device efficiencies of CTMC-based neat-film LECs.

Results and discussions

Photoluminescent studies

Molecular structures of the CTMC and the carrier trapper used in this study are shown in Fig. 1. The cyan-emitting CTMC [Ir(dfppz)$_2$(dtb-bpy)]$^+$(PF_6^-) (where dfppz is 1-(2,4-difluorophenyl) pyrazole and dtb-bpy is [4,4′-di(*tert*-butyl)-2,2′-bipyridine]) reported previously by Tamayo *et al.*[29] was used as the emissive material. [Ir(dfppz)$_2$(dtb-bpy)]$^+$(PF_6^-) was synthesized according to the procedures reported in the literature.[29] The cationic fluorescent NIR laser dye 3,3′-diethyl-2,2′-oxathiacarbocyanine iodide (DOTCI), which has been reported as an active material in efficient NIR dye lasers,[62] was utilized as the carrier trapper. DOTCI was purchased from Sigma-Aldrich Co. and was used as received. The PL spectrum of the [Ir(dfppz)$_2$(dtb-bpy)]$^+$(PF_6^-) neat films and absorption/PL spectra of DOTCI in dilute ethanol solutions are shown in Fig. 2. Neat films of [Ir(dfppz)$_2$(dtb-bpy)]$^+$(PF_6^-) exhibit cyan phosphorescent PL centered at 490 nm. Highly retained PLQY of [Ir(dfppz)$_2$(dtb-bpy)]$^+$(PF_6^-) in neat films (0.75)[59] in comparison with that in dilute solutions (1.00)[59] reveals reduced self-quenching in neat films possibly resulting from the sterically bulky di-*tert*-butyl groups of the bipyridine ligand,[29] suggesting its suitability for use as the emissive material of neat-film LECs. DOTCI in ethanol solutions (10^{-5} M) exhibits concentrated NIR PL spectra centered at 720 nm. It is noted that since the absorption spectrum of DOTCI

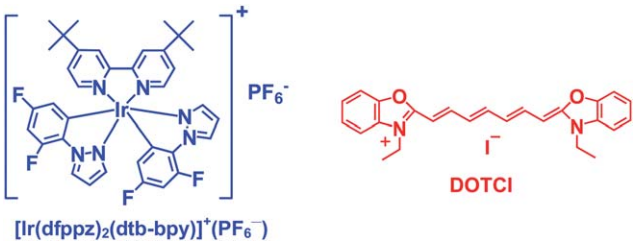

Fig. 1 Molecular structures of the CTMC [Ir(dfppz)$_2$(dtb-bpy)]$^+$(PF_6^-) and the carrier trapper DOTCI.

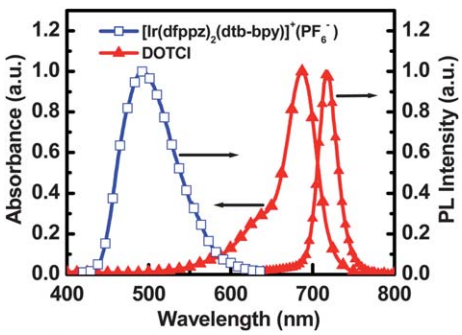

Fig. 2 PL spectrum of the [Ir(dfppz)$_2$(dtb-bpy)]$^+$(PF_6^-) neat film and absorption/PL spectra of DOTCI in ethanol solution (10^{-5} M).

and the PL spectrum of $[Ir(dfppz)_2(dtb\text{-}bpy)]^+(PF_6^-)$ exhibit poor spectral overlap (Fig. 2), inefficient energy transfer between them would be expected. Thus, significant DOTCI emission in the NIR region, which would lead to a considerable color shift in the $[Ir(dfppz)_2(dtb\text{-}bpy)]^+(PF_6^-)$ emission, would be prevented at low DOTCI doping concentrations. However, even at low DOTCI doping concentrations, the large offset in the energy levels between $[Ir(dfppz)_2(dtb\text{-}bpy)]^+(PF_6^-)$ and DOTCI would still be effective to induce significant carrier trapping and consequently result in an altered balance of carrier mobilities.

Doping of the carrier trapper DOTCI in $[Ir(dfppz)_2(dtb\text{-}bpy)]^+(PF_6^-)$ neat films to modify the balance of carrier mobilities may simultaneously lead to additional DOTCI emission, which deteriorates color purity of the $[Ir(dfppz)_2(dtb\text{-}bpy)]^+(PF_6^-)$ emission. To clarify the energy transfer properties between $[Ir(dfppz)_2(dtb\text{-}bpy)]^+(PF_6^-)$ and DOTCI, Fig. 3 depicts the PL spectra of the $[Ir(dfppz)_2(dtb\text{-}bpy)]^+(PF_6^-)$ films containing various concentrations of DOTCI. The excitation wavelength is 365 nm, at which the absorption of $[Ir(dfppz)_2(dtb\text{-}bpy)]^+(PF_6^-)$ is much higher than that of DOTCI at low doping concentrations, minimizing direct absorption of DOTCI and thus ensuring DOTCI emission mainly coming from energy transfer. Since in LECs, an ionic liquid $BMIM^+(PF_6^-)$ (where BMIM is 1-butyl-3-methylimidazolium) of 20 wt% was added to provide additional mobile ions and to shorten the device response time,[27] PL properties of the $BMIM^+(PF_6^-)$ (20 wt%) blended films were characterized. With the increase of the DOTCI concentration, the relative intensity of the DOTCI emission with respect to the $[Ir(dfppz)_2(dtb\text{-}bpy)]^+(PF_6^-)$ emission is larger due to a relatively higher energy transfer rate at a higher DOTCI concentration. However, it is noted that the DOTCI emission is weak at low DOTCI concentrations (0.01–0.1 wt%) and the PL spectra are predominantly the $[Ir(dfppz)_2(dtb\text{-}bpy)]^+(PF_6^-)$ emission, confirming inefficient energy transfer in the $[Ir(dfppz)_2(dtb\text{-}bpy)]^+(PF_6^-)$/DOTCI system at such low DOTCI concentrations. Hence, color shift in the $[Ir(dfppz)_2(dtb\text{-}bpy)]^+(PF_6^-)$ emission induced by dilute doping of DOTCI for tailoring the balance of carrier mobilities would not be significant.

EL characteristics of the LEC devices

To study the EL properties of the LECs doped with a carrier trapper, the EL characteristics of the LECs based on $[Ir(dfppz)_2(dtb\text{-}bpy)]^+(PF_6^-)$ containing various concentrations of DOTCI were measured and are summarized in Table 1. The LECs have the structure of indium tin oxide (ITO)/poly(3,4-ethylenedioxythiophene):poly(styrene sulfonate) (PEDOT:PSS) (30 nm)/emissive layer (200 nm)/Ag (100 nm), where the emissive layer contains $[Ir(dfppz)_2(dtb\text{-}bpy)]^+(PF_6^-)$ [$(80 - x)$ wt%], DOTCI (x wt%) and $BMIM^+(PF_6^-)$ (20 wt%) and $x = 0$, 0.01, 0.1 and 1 for **Devices I**, **II**, **III**, and **IV**, respectively. The ionic liquid $BMIM^+(PF_6^-)$ was added to provide additional mobile ions and to shorten the device response time.[27] The EL spectra of the LECs based on $[Ir(dfppz)_2(dtb\text{-}bpy)]^+(PF_6^-)$ containing various concentrations of DOTCI and $BMIM^+(PF_6^-)$ (20 wt%) at 3.3 V are shown in Fig. 4. For the emission coming from $[Ir(dfppz)_2(dtb\text{-}bpy)]^+(PF_6^-)$, EL spectra are basically similar to PL spectra, indicating similar emission mechanisms. However, the relative intensity of the DOTCI emission with respect to the $[Ir(dfppz)_2(dtb\text{-}bpy)]^+(PF_6^-)$ emission in EL (Fig. 4) is smaller than that in PL (Fig. 3) at the same DOTCI concentration. This phenomenon would be explained as follows. The PL emission of DOTCI (Fig. 3) mainly comes from the Förster energy transfer[63]

Table 1 Summary of the LEC device characteristics

Device (DOTCI concentration)	Bias/V	t_{max}[a]/ min	L_{max}[b]/ cd m^{-2}	$\eta_{ext,\ max}$[c] (%)	$\eta_{p,\ max}$[d]/ lm W^{-1}	$t_{1/2}$[e]/ min
I (0.0 wt%)	3.3	49	10.94	9.06	19.14	40
	3.5	32	19.41	8.54	16.78	24
	3.7	23	25.21	7.51	13.96	15
II (0.01 wt%)	3.3	62	16.62	12.75	28.70	45
	3.5	34	24.48	12.30	26.53	27
	3.7	25	42.50	11.27	22.12	16
III (0.1 wt%)	3.3	68	6.03	6.94	15.06	48
	3.5	54	11.03	6.62	13.53	31
	3.7	28	14.00	6.55	12.36	18
IV (1.0 wt%)	3.3	295	0.95	0.72	1.56	233
	3.5	161	1.86	0.74	1.46	53
	3.7	119	2.78	0.73	1.27	23

[a] Time required to reach the maximal brightness. [b] Maximal brightness achieved at a constant bias voltage. [c] Maximal external quantum efficiency achieved at a constant bias voltage. [d] Maximal power efficiency achieved at a constant bias voltage. [e] The time for the brightness of the device to decay from the maximum to half of the maximum under a constant bias voltage.

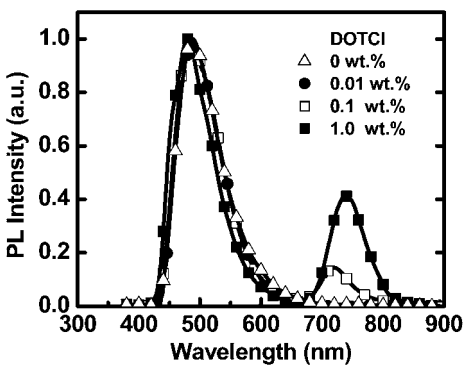

Fig. 3 PL spectra of the $[Ir(dfppz)_2(dtb\text{-}bpy)]^+(PF_6^-)$ films containing various concentrations of DOTCI and $BMIM^+(PF_6^-)$ (20 wt%).

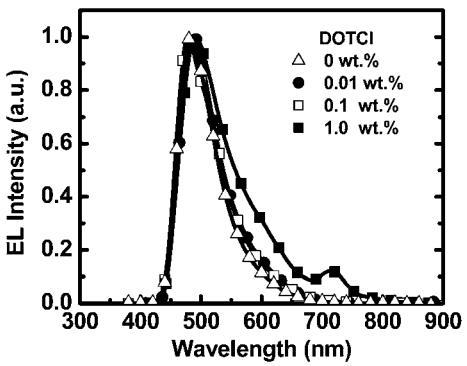

Fig. 4 EL spectra of the LECs based on $[Ir(dfppz)_2(dtb\text{-}bpy)]^+(PF_6^-)$ containing various concentrations of DOTCI and $BMIM^+(PF_6^-)$ (20 wt %) at 3.3 V.

from triplet excitons of $[Ir(dfppz)_2(dtb\text{-}bpy)]^+(PF_6^-)$ to singlet excitons of DOTCI. Dexter energy transfer[64] from triplet excitons of $[Ir(dfppz)_2(dtb\text{-}bpy)]^+(PF_6^-)$ to triplet excitons of DOTCI, which decay nonradiatively, would be insignificant when the pumping level (and thus the concentration of triplet excitons) is low.[65] For host–guest LECs, electrochemically doped regions of the emissive layer result in ohmic contacts with metal electrodes and consequently facilitate carrier injection onto both the host and the guest. Hence, both exciton formation on the host followed by host–guest energy transfer (Förster and/or Dexter energy transfer) and direct exciton formation on the guest induced by carrier trapping contribute to the guest emission. Direct exciton formation on the guest would be significant in a host–guest system exhibiting large offsets in the energy levels between the host and the guest since carrier trapping would be facilitated by such energy level alignment. The energy level diagram of $[Ir(dfppz)_2(dtb\text{-}bpy)]^+(PF_6^-)$ and DOTCI estimated by cyclic voltammetry is shown in the inset of Fig. 5. A large energy offset (1.36 eV) in the HOMO levels between $[Ir(dfppz)_2(dtb\text{-}bpy)]^+(PF_6^-)$ and DOTCI would lead to significant hole trapping. The maximum current density *versus* voltage characteristics of LECs based on $[Ir(dfppz)_2(dtb\text{-}bpy)]^+(PF_6^-)$ containing various concentrations of DOTCI and $BMIM^+(PF_6^-)$ (20 wt%) are shown in Fig. 5. The maximum device current density under the same bias voltage decreases as the concentration of DOTCI increases and thus confirms significant carrier trapping, resulting in direct exciton formation on DOTCI. As a result, only singlet excitons (~25% of total excitons directly formed on DOTCI) contribute to the EL emission from DOTCI (Fig. 4). Triplet excitons (~75% of total excitons directly formed on DOTCI) cannot be harvested due to the spin selection rule. On the other hand, Dexter energy transfer may not be ignored in devices under electrical driving, in which the concentration of triplet excitons would be higher than that in thin films under illumination of low-power UV light. Dexter energy transfer takes place between host triplets and guest triplets, which decay nonradiatively, when the concentration of host triplets increases and thus would degrade the EL efficiency of phosphorescent sensitized (phosphorescent host doped with fluorescent guest) LECs.[56] Thus, it would be responsible for the lower relative intensity of the DOTCI emission with respect to the $[Ir(dfppz)_2(dtb\text{-}bpy)]^+(PF_6^-)$ emission in EL (Fig. 4) as compared to that in PL (Fig. 3). These results reveal that doping of DOTCI in $[Ir(dfppz)_2(dtb\text{-}bpy)]^+(PF_6^-)$ films at concentrations lower than 0.1 wt% renders almost unaffected EL spectra of $[Ir(dfppz)_2(dtb\text{-}bpy)]^+(PF_6^-)$ (Fig. 4) while carrier trapping induced by DOTCI at such low concentrations (Fig. 5) would still significantly modify the balance of carrier mobilities in the LEC devices.

The LECs based on $[Ir(dfppz)_2(dtb\text{-}bpy)]^+(PF_6^-)$ doped with various DOTCI concentrations and $BMIM^+(PF_6^-)$ (20 wt%) exhibited similar time-dependent EL characteristics under constant-bias operation. Fig. 6(a) shows the time-dependent brightness and current density under constant biases of 3.3–3.7 V for **Device II**. After the bias was applied, the current first increased and then stayed rather constant. On the other hand, the brightness first increased with the current and reached the maxima of 16.62, 24.28 and 42.50 cd m^{-2} under biases of 3.3, 3.5 and 3.7 V, respectively. The brightness then dropped with time with a rate depending on the bias voltage (or current). Corresponding time-dependent EQEs and power efficiencies of the same device are shown in Fig. 6(b). When a forward bias was just applied, the EQE was rather low due to poor carrier injection. During the formation of the p- and n-type regions near electrodes, the capability of carrier injection was improved and the EQE thus rose rapidly. The peak EQE and the peak power efficiencies at 3.3, 3.5 and 3.7 V are 12.75% and 28.70 lm W^{-1}, 12.30% and 26.53 lm W^{-1} and 11.27% and 22.12 lm W^{-1}, respectively. The drop of device efficiency after reaching the peak value, as commonly seen in solid-state LECs,[11–60] may be associated with a few factors. Before the device current reaches

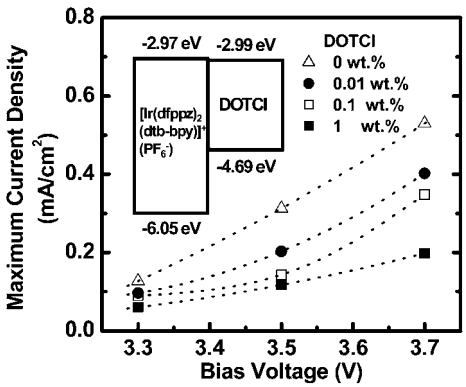

Fig. 5 Maximum current density *vs.* voltage characteristics for the LECs based on $[Ir(dfppz)_2(dtb\text{-}bpy)]^+(PF_6^-)$ containing various concentrations of DOTCI and $BMIM^+(PF_6^-)$ (20 wt%). Inset: the energy level diagram of $[Ir(dfppz)_2(dtb\text{-}bpy)]^+(PF_6^-)$ and DOTCI molecules.

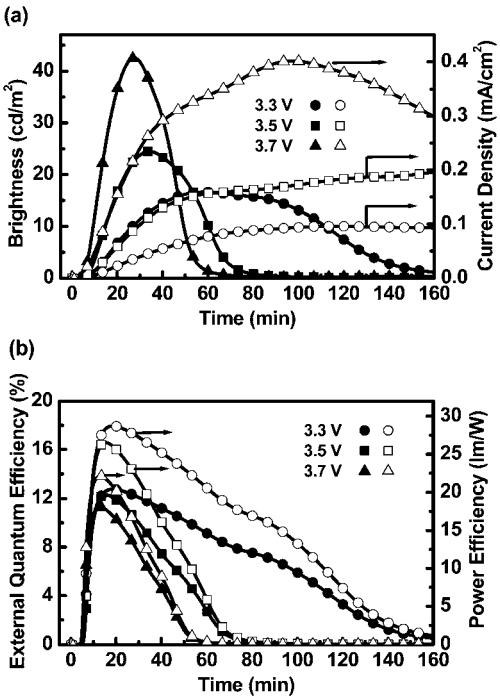

Fig. 6 (a) Brightness (solid symbols) and current density (open symbols) and (b) external quantum efficiency (solid symbols) and power efficiency (open symbols) as a function of time under a constant bias voltage of 3.3–3.7 V for **Device II**.

a steady value, the carrier recombination zone may keep moving closer to one electrode due to a discrepancy in electron and hole mobilities, which would induce exciton quenching such that the device efficiency would decrease with time while the current and the brightness are still increasing. Further, the decrease in brightness and efficiency under a relatively steady device current may be rationally attributed to the degradation of the emissive material during the LEC operation.[21]

Peak EQEs and peak power efficiencies (at current densities < 0.1 mA cm^{-2}) of the LECs based on $[Ir(dfppz)_2(dtb\text{-}bpy)]^+(PF_6^-)$ doped with various DOTCI concentrations and $BMIM^+(PF_6^-)$ (20 wt%) are shown in Fig. 7. The device efficiency first increases, then decreases as the DOTCI concentration increases from 0 to 1 wt%. The undoped LECs based on $[Ir(dfppz)_2(dtb\text{-}bpy)]^+(PF_6^-)$ show an EQE up to 9.06%. However, this result is much lower than the upper limit (~15%) that one would expect from the PLQY of the emissive layer (~0.75)[59] and an optical outcoupling efficiency of ~20% from a typical layered light-emitting device structure. Since the electrochemically doped regions near electrodes of LECs ensure balanced carrier injection,[1,2] such lowered device efficiency would be attributed to the imperfect balance of carrier mobilities in the $[Ir(dfppz)_2(dtb\text{-}bpy)]^+(PF_6^-)$ films. As the carrier injection at both electrodes is becoming balanced, the carrier recombination zone may consequently locate near one of the electrodes due to discrepancy in electron and hole mobilities of the emissive layer. The recombination zone in the vicinity of an electrode may cause exciton quenching such that the EQE of the device would decrease. The ppz-based complex $Ir(ppz)_3$ (where ppz is 1-phenylpyrazole) has been reported to be a hole transporting/electron blocking material.[66] Furthermore, the cationic complex $[Ir(dfppy)_2(bpy)]^+(PF_6^-)$ (where dfppy is 2-(2,4-difluorophenyl) pyridine and bpy is 2,2′-bipyridine) was shown to exhibit higher hole mobility than electron mobility.[67] Thus, a similar complex $[Ir(dfppz)_2(dtb\text{-}bpy)]^+(PF_6^-)$ containing ppz and bpy moieties would also prefer hole transport. The suggested schematic diagram of the position of the exciton recombination zone for the LECs based on $[Ir(dfppz)_2(dtb\text{-}bpy)]^+(PF_6^-)$ and $BMIM^+(PF_6^-)$ (20 wt%) is depicted in Fig. 8(a). The exciton recombination zone approaching the cathode leads to exciton quenching and thus deteriorates the device efficiency. To balance the carrier mobilities for moving the exciton recombination zone toward the center of the emissive layer, a low-gap carrier trapper DOTCI is doped in the $[Ir(dfppz)_2(dtb\text{-}bpy)]^+(PF_6^-)$ films. A large energy offset

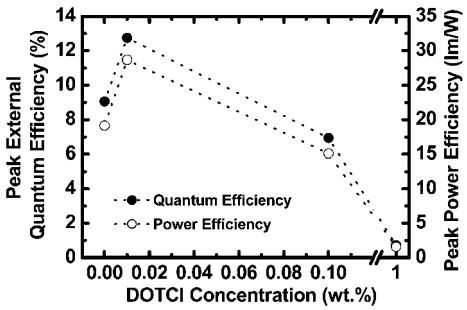

Fig. 7 Peak external quantum efficiencies and peak power efficiencies (at current densities < 0.2 mA cm^{-2}) of the LECs as a function of the DOTCI concentration.

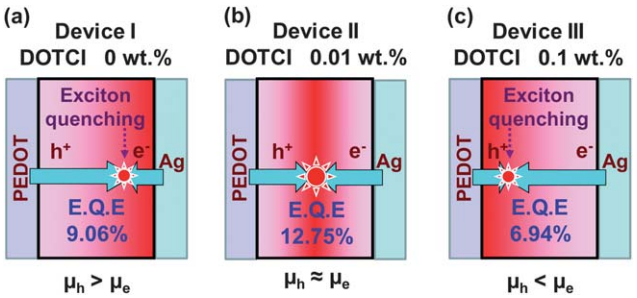

Fig. 8 Schematic diagrams of the position of the exciton recombination zone for (a) **Device I**, (b) **Device II** and (c) **Device III**. Electrochemically doped regions near electrodes are omitted for clarity.

(1.36 eV) in the HOMO levels between $[Ir(dfppz)_2(dtb\text{-}bpy)]^+(PF_6^-)$ and DOTCI (the inset of Fig. 5) impedes hole transport in the emissive layer. On the other hand, similar energies in the LUMO levels of $[Ir(dfppz)_2(dtb\text{-}bpy)]^+(PF_6^-)$ and DOTCI (the inset of Fig. 5) keep the electron mobilities of the emissive layer relatively unchanged. As a result, doping of DOTCI would improve the balance of carrier mobilities in $[Ir(dfppz)_2(dtb\text{-}bpy)]^+(PF_6^-)$ films and consequently move the exciton recombination zone toward the center of the emissive layer (Fig. 8(b)), improving the device efficiencies. With the DOTCI concentration of 0.01 wt%, the peak EQE and the peak power efficiency of the LECs reach 12.75% and 28.70 lm W^{-1}, respectively (Fig. 7). Such device efficiencies are enhanced by 1.4 times as compared to those of the undoped devices and approach the upper limit (~15%) that one would expect from the PLQY of the emissive layer (~0.75)[59] and an optical outcoupling efficiency of ~20% from a typical layered light-emitting device structure. These results confirm characteristics of preferred transport of hole for $[Ir(dfppz)_2(dtb\text{-}bpy)]^+(PF_6^-)$ and the improved balance of carrier mobilities in the doped emissive layer. To the best of our knowledge, these device efficiencies are among the highest reported values for neat-film cyan emitting LECs. Further increasing the concentration of DOTCI would result in over-modified hole mobilities and thus deteriorate the balance of carrier mobilities as well (Fig. 8(c)). With the DOTCI concentration of 0.1 wt%, severe hole trapping leads to lower hole mobility compared with electron mobility and the exciton recombination zone would be pushed toward the anode in consequence. Exciton quenching near the anode also causes a deteriorated EQE of 6.94% (Fig. 7). These results reveal that doping of a proper carrier trapper in CTMC neat films would modify the balance of carrier mobilities of the emissive layer and thus enhance device efficiencies of neat-film LECs.

The turn-on time (the time required to reach the maximal brightness) as a function of bias voltage for LECs is shown in Fig. 9(a). An electrochemical junction between p- and n-type doped layers of LECs is formed during device operation. The higher electric field in the device induced by a higher bias voltage accelerates redistribution of mobile ions, which facilitates formation of ohmic contacts with the electrodes and thus fastens the device response. It is noted that the turn-on time of the LECs under the same bias voltage increases as the DOTCI concentration increases. More pronounced carrier trapping in LECs with higher DOTCI concentrations decreases the effective bias voltage across the emissive layer and consequently leads to

a lower electric field, rendering a slower device response under the same bias voltage. Carrier trapping induced by doping of DOTCI also decreases the device current density (Fig. 5) and thus is beneficial in device stability. As shown in Fig. 9(b), the device lifetime (the time for the brightness of the device to decay from the maximum to half of the maximum under a constant bias voltage) of LECs increases as the DOTCI concentration increases. It may be associated with the fact that the lower electric field or current density decelerates degradation (multiple oxidation and subsequent decomposition)[27] of the CTMC materials. Detailed degradation mechanisms of LECs based on CTMCs remain unclear and further studies are still needed to achieve practical device lifetimes. Recently published literature[60] revealed that device current and brightness of sandwiched LECs first increase with extension of the p- and n-type electrochemically doped regions. As the width of the doping layers increases, the width of the neutral layer decreases and thus the number of excitons being quenched increases, leading to reduced brightness. Adding a hole trapper to decrease the hole mobility would reduce the speed of formation of the p-type doped layer and thus would slow down the evolution rate of the device current and brightness, leading to lengthened turn-on times and lifetimes. Our observed results are consistent with the reported model of LECs.[60]

Conclusions

In this work, we demonstrate improvements in the balance of carrier mobilities in neat-film LECs utilizing a cyan-emitting phosphorescent CTMC $[Ir(dfppz)_2(dtb\text{-}bpy)]^+(PF_6^-)$ as the emissive material and a cationic fluorescent NIR laser dye DOTCI as the carrier trapper. This low-gap carrier trapper is chosen such that a significant energy offset in the HOMO levels between $[Ir(dfppz)_2(dtb\text{-}bpy)]^+(PF_6^-)$ and DOTCI impedes hole transport in the emissive layers while similar LUMO levels of these two materials result in a relatively unaffected electron transport. Therefore, the balance of carrier mobilities in the CTMC neat films, which would intrinsically exhibit characteristics of preferred transport of holes, would be improved by doping such carrier trapper. PL measurements reveal inefficient energy transfer between $[Ir(dfppz)_2(dtb\text{-}bpy)]^+(PF_6^-)$ and DOTCI due to poor spectral overlap between the $[Ir(dfppz)_2(dtb\text{-}bpy)]^+(PF_6^-)$ emission and DOTCI absorption, ensuring unapparent DOTCI emission and thus reducing color shift in the $[Ir(dfppz)_2(dtb\text{-}bpy)]^+(PF_6^-)$ emission at low doping concentrations of DOTCI. However, even at low doping concentrations, carrier trapping would still be effective due to the large energy offset in the HOMO levels between $[Ir(dfppz)_2(dtb\text{-}bpy)]^+(PF_6^-)$ and DOTCI. EL measurements show that the peak EQE (power efficiency) of the neat-film LECs doped with the carrier trapper reaches 12.75% (28.70 lm W^{-1}), representing a 1.4 times enhancement in device efficiency as compared to that of the undoped neat-film LECs. Such device efficiency approaches the upper limit (~15%) that one would expect from the PLQY of the emissive layer (~0.75) and an optical outcoupling efficiency of ~20% from a typical layered light-emitting device structure, consequently indicating superior balance of carrier mobilities in such doped emissive layer. These results confirm the strategy of introducing a proper carrier trapper into the CTMC neat films would improve the balance of carrier mobilities in the emissive layer, offering a general approach for optimizing device efficiencies of CTMC-based neat-film LECs.

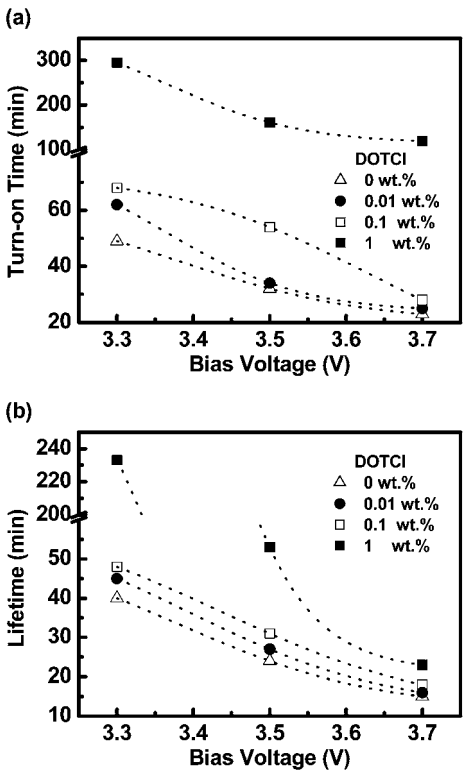

Fig. 9 (a) Turn-on time and (b) lifetime as a function of bias voltage for the LECs based on $[Ir(dfppz)_2(dtb\text{-}bpy)]^+(PF_6^-)$ containing various concentrations of DOTCI and $BMIM^+(PF_6^-)$ (20 wt%).

Experimental

Photoluminescent characterization

The mixed films for PL studies were spin-coated at 3000 rpm onto quartz substrates (1 × 0.5 cm^2) using mixed solutions (in acetonitrile) of various ratios. Since in LECs, an ionic liquid $BMIM^+(PF_6^-)$ of 20 wt% was added to provide additional mobile ions and to shorten the device response time,[27] PL properties of the $BMIM^+(PF_6^-)$ blended films were characterized. The mass ratio of solute component of $[Ir(dfppz)_2(dtb\text{-}bpy)]^+(PF_6^-)$, DOTCI and $BMIM^+(PF_6^-)$ in acetonitrile solutions for spin coating of the mixed films is $(80 - x)$, x and 20, respectively ($x = 0$, 0.01, 0.1, 1). The concentrations of all solutions for spin coating are 80 mg mL^{-1}. The thickness of each spin-coated film was *ca.* 200 nm, as measured using profilometry. UV-Vis absorption spectra were recorded using a Hitachi U2800A spectrophotometer. PL spectra were recorded using a Hitachi F9500 fluorescence spectrophotometer. PLQYs for thin-film samples were determined with a calibrated integrating sphere system (HAMAMATSU C9920).

LEC device fabrication and characterization

ITO-coated glass substrates (2 × 2 cm^2) were cleaned and treated with UV/ozone prior to use. A PEDOT:PSS layer was

spin-coated at 4000 rpm onto the ITO substrate in air and baked at 150 °C for 30 min. The emissive layer (~200 nm, as measured by profilometry) was then spin-coated at 3000 rpm from mixed acetonitrile solutions. The mass ratio of solute component and the concentrations of solutions for spin coating of the emissive layers were the same as those used for spin coating of the mixed films containing $BMIM^+(PF_6^-)$ for PL studies described above. The ionic liquid $[BMIM^+(PF_6)^-]$ was added to enhance the ionic conductivity of thin films and thus to reduce the turn-on time of the LEC device.[27] All solution preparing and spin-coating processes were carried out under ambient conditions. After spin coating, the thin films were then baked at 70 °C for 10 hours in a nitrogen glove box (oxygen and moisture levels below 1 ppm), followed by thermal evaporation of a 100 nm Ag top contact in a vacuum chamber (~10^{-6} Torr). The electrical and emission characteristics of LEC devices were measured using a source-measurement unit and a Si photodiode calibrated with the Photo Research PR-650 spectroradiometer. All device measurements were performed under a constant bias voltage (3.3–3.7 V) in a nitrogen glove box. The EL spectra were taken with a calibrated CCD spectrograph.

Acknowledgements

The authors gratefully acknowledge the financial support from the National Science Council of Taiwan.

References

1 Q. Pei, G. Yu, C. Zhang, Y. Yang and A. J. Heeger, *Science*, 1995, **269**, 1086.
2 Q. Pei, Y. Yang, G. Yu, C. Zhang and A. J. Heeger, *J. Am. Chem. Soc.*, 1996, **118**, 3922.
3 E. Tekin, E. Holder, V. Marin, B.-J. de Gans and U. S. Schubert, *Macromol. Rapid Commun.*, 2005, **26**, 293.
4 V. Marin, E. Holder, M. M. Wienk, E. Tekin, D. Kozodaev and U. S. Schubert, *Macromol. Rapid Commun.*, 2005, **26**, 319.
5 E. Tekin, H. Wijlaars, E. Holder, D. A. M. Egbe and U. S. Schubert, *J. Mater. Chem.*, 2006, **16**, 4294.
6 C. W. Tang and S. A. VanSlyke, *Appl. Phys. Lett.*, 1987, **51**, 913.
7 C. W. Tang, S. A. VanSlyke and C. H. Chen, *Appl. Phys. Lett.*, 1989, **65**, 3610.
8 C. Ulbricht, N. Rehmann, E. Holder, D. Hertel, K. Meerholz and U. S. Schubert, *Macromol. Chem. Phys.*, 2009, **210**, 531.
9 N. Tian, A. Thiessen, R. Schiewek, O. J. Schmitz, D. Hertel, K. Meerholz and E. Holder, *J. Org. Chem.*, 2009, **74**, 2718.
10 N. Rehmann, C. Ulbricht, A. Köhnen, P. Zacharias, M. C. Gather, D. Hertel, E. Holder, K. Meerholz and U. S. Schubert, *Adv. Mater.*, 2008, **20**, 129.
11 J. K. Lee, D. S. Yoo, E. S. Handy and M. F. Rubner, *Appl. Phys. Lett.*, 1996, **69**, 1686.
12 C. H. Lyons, E. D. Abbas, J. K. Lee and M. F. Rubner, *J. Am. Chem. Soc.*, 1998, **120**, 12100.
13 F. G. Gao and A. J. Bard, *J. Am. Chem. Soc.*, 2000, **122**, 7426.
14 E. Holder, G. Schoetz, V. Schurig and E. Lindner, *Tetrahedron: Asymmetry*, 2001, **12**, 2289.
15 E. Holder, M. A. R. Meier, V. Marin and U. S. Schubert, *J. Polym. Sci., Part A: Polym. Chem.*, 2003, **41**, 3954.
16 V. Marin, E. Holder and U. S. Schubert, *J. Polym. Sci., Part A: Polym. Chem.*, 2004, **42**, 374.
17 V. Marin, E. Holder, R. Hoogenboom and U. S. Schubert, *J. Polym. Sci., Part A: Polym. Chem.*, 2004, **42**, 4153.
18 E. Holder, V. Marin, A. Alexeev and U. S. Schubert, *J. Polym. Sci., Part A: Polym. Chem.*, 2005, **43**, 2765.
19 H. Rudmann and M. F. Rubner, *J. Appl. Phys.*, 2001, **90**, 4338.
20 H. Rudmann, S. Shimada and M. F. Rubner, *J. Am. Chem. Soc.*, 2002, **124**, 4918.
21 G. Kalyuzhny, M. Buda, J. McNeill, P. Barbara and A. J. Bard, *J. Am. Chem. Soc.*, 2003, **125**, 6272.
22 J. D. Slinker, D. Bernards, P. L. Houston, H. D. Abruña, S. Bernhard and G. G. Malliaras, *Chem. Commun.*, 2003, 2392.
23 H. Rudmann, S. Shimada and M. F. Rubner, *J. Appl. Phys.*, 2003, **94**, 115.
24 J. D. Slinker, A. A. Gorodetsky, M. S. Lowry, J. Wang, S. Parker, R. Rohl, S. Bernhard and G. G. Malliaras, *J. Am. Chem. Soc.*, 2004, **126**, 2763.
25 A. R. Hosseini, C. Y. Koh, J. D. Slinker, S. Flores-Torres, H. D. Abruña and G. G. Malliaras, *Chem. Mater.*, 2005, **17**, 6114.
26 J. D. Slinker, C. Y. Koh, G. G. Malliaras, M. S. Lowry and S. Bernhard, *Appl. Phys. Lett.*, 2005, **86**, 173506.
27 S. T. Parker, J. D. Slinker, M. S. Lowry, M. P. Cox, S. Bernhard and G. G. Malliaras, *Chem. Mater.*, 2005, **17**, 3187.
28 M. S. Lowry, J. I. Goldsmith, J. D. Slinker, R. Rohl, R. A. Pascal, Jr, G. G. Malliaras and S. Bernhard, *Chem. Mater.*, 2005, **17**, 5712.
29 A. B. Tamayo, S. Garon, T. Sajoto, P. I. Djurovich, I. M. Tsyba, R. Bau and M. E. Thompson, *Inorg. Chem.*, 2005, **44**, 8723.
30 N. Armaroli, G. Accorsi, M. Holler, O. Moudam, J. Nierengarten, Z. Zhou, R. T. Wegh and R. Welter, *Adv. Mater.*, 2006, **18**, 1313.
31 H. J. Bolink, L. Cappelli, E. Coronado, M. Grätzel and M. Nazeeruddin, *J. Am. Chem. Soc.*, 2006, **128**, 46.
32 H. J. Bolink, L. Cappelli, E. Coronado, M. Grätzel, E. Ortí, R. D. Costa, P. M. Viruela and M. Nazeeruddin, *J. Am. Chem. Soc.*, 2006, **128**, 14786.
33 Q. Zhang, Q. Zhou, Y. Cheng, L. Wang, D. Ma, X. Jing and F. Wang, *Adv. Funct. Mater.*, 2006, **16**, 1203.
34 M. K. Nazeeruddin, R. T. Wegh, Z. Zhou, C. Klein, Q. Wang, F. De Angelis, S. Fantacci and M. Grätzel, *Inorg. Chem.*, 2006, **45**, 9245.
35 H. J. Bolink, L. Cappelli, E. Coronado, A. Parham and P. Stössel, *Chem. Mater.*, 2006, **18**, 2778.
36 H.-C. Su, F.-C. Fang, T.-Y. Hwu, H.-H. Hsieh, H.-F. Chen, G.-H. Lee, S.-M. Peng, K.-T. Wong and C.-C. Wu, *Adv. Funct. Mater.*, 2007, **17**, 1019.
37 H.-C. Su, C.-C. Wu, F.-C. Fang and K.-T. Wong, *Appl. Phys. Lett.*, 2006, **89**, 261118.
38 J. D. Slinker, J. Rivnay, J. S. Moskowitz, J. B. Parker, S. Bernhard, H. D. Abruña and G. G. Malliaras, *J. Mater. Chem.*, 2007, **17**, 2976.
39 L. He, L. Duan, J. Qiao, R. Wang, P. Wei, L. D. Wang and Y. Qiu, *Adv. Funct. Mater.*, 2008, **18**, 2123.
40 E. Z. Colman, J. D. Slinker, J. B. Parker, G. G. Malliaras and S. Bernhard, *Chem. Mater.*, 2008, **20**, 388.
41 H.-C. Su, H.-F. Chen, F.-C. Fang, C.-C. Liu, C.-C. Wu, K.-T. Wong, Y.-H. Liu and S.-M. Peng, *J. Am. Chem. Soc.*, 2008, **130**, 3413.
42 S. Graber, K. Doyle, M. Neuburger, C. E. Housecroft, E. C. Constable, R. D. Costa, E. Ortí, D. Repetto and H. J. Bolink, *J. Am. Chem. Soc.*, 2008, **130**, 14944.
43 H. J. Bolink, E. Coronado, R. D. Costa, E. Ortí, M. Sessolo, S. Graber, K. Doyle, M. Neuburger, C. E. Housecroft and E. C. Constable, *Adv. Mater.*, 2008, **20**, 3910.
44 H. J. Bolink, E. Coronado, R. D. Costa, N. Lardiés and E. Ortí, *Inorg. Chem.*, 2008, **47**, 9149.
45 H.-C. Su, H.-F. Chen, C.-C. Wu and K.-T. Wong, *Chem.–Asian J.*, 2008, **3**, 1922.
46 T.-H. Kwon, Y. H. Oh, I.-S. Shin and J.-I. Hong, *Adv. Funct. Mater.*, 2009, **19**, 711.
47 L. He, J. Qiao, L. Duan, G. F. Dong, D. Q. Zhang, L. D. Wang and Y. Qiu, *Adv. Funct. Mater.*, 2009, **19**, 2950.
48 C. Rothe, C.-J. Chiang, V. Jankus, K. Abdullah, X. Zeng, R. Jitchati, A. S. Batsanov, M. R. Bryce and A. P. Monkman, *Adv. Funct. Mater.*, 2009, **19**, 2038.
49 R. D. Costa, E. Ortí, H. J. Bolink, S. Graber, S. Schaffner, M. Neuburger, C. E. Housecroft and E. C. Constable, *Adv. Funct. Mater.*, 2009, **19**, 3456.
50 R. D. Costa, E. Ortí, H. J. Bolink, S. Graber, C. E. Housecroft, M. Neuburger, S. Schaffnerb and E. C. Constable, *Chem. Commun.*, 2009, 2029.
51 R. D. Costa, F. J. Céspedes-Guirao, E. Ortí, H. J. Bolink, J. Gierschner, F. Fernández-Lázaro and A. Sastre-Santos, *Chem. Commun.*, 2009, 3886.
52 L. He, L. Duan, J. Qiao, G. Dong, L. Wang and Y. Qiu, *Chem. Mater.*, 2010, **22**, 3535.
53 R. D. Costa, E. Ortí, H. J. Bolink, S. Graber, C. E. Housecroft and E. C. Constable, *J. Am. Chem. Soc.*, 2010, **132**, 5978.

54 R. D. Costa, E. Ortí, H. J. Bolink, S. Graber, C. E. Housecroft and E. C. Constable, *Adv. Funct. Mater.*, 2010, **20**, 1511.
55 M. Mydlak, C. Bizzarri, D. Hartmann, W. Sarfert, G. Schmid and L. De Cola, *Adv. Funct. Mater.*, 2010, **20**, 1812.
56 H.-C. Su, Y.-H. Lin, C.-H. Chang, H.-W. Lin, C.-C. Wu, F.-C. Fang, H.-F. Chen and K.-T. Wong, *J. Mater. Chem.*, 2010, **20**, 5521.
57 C.-H. Yang, J. Beltran, V. Lemaur, J. Cornil, D. Hartmann, W. Sarfert, R. Fröhlich, C. Bizzarri and L. De Cola, *Inorg. Chem.*, 2010, **49**, 9891.
58 H.-F. Chen, K.-T. Wong, Y.-H. Liu, Y. Wang, Y.-M. Cheng, M.-W. Chung, P.-T. Chou and H.-C. Su, *J. Mater. Chem.*, 2011, **21**, 768.
59 H.-C. Su, H.-F. Chen, Y.-C. Shen, C.-T. Liao and K.-T. Wong, *J. Mater. Chem.*, 2011, **21**, 9653.
60 M. Lenes, G. Garcia-Belmonte, D. Tordera, A. Pertegás, J. Bisquert and H. J. Bolink, *Adv. Funct. Mater.*, 2011, **21**, 1581.
61 K. W. Lee, J. D. Slinker, A. A. Gorodetsky, S. Flores-Torres, H. D. Abruña, P. L. Houston and G. G. Malliaras, *Phys. Chem. Chem. Phys.*, 2003, **5**, 2706.
62 P. F. Aramendia, R. M. Negri and E. S. Roman, *J. Phys. Chem.*, 1994, **98**, 3165.
63 T. Förster, *Discuss. Faraday Soc.*, 1959, **27**, 7.
64 D. L. Dexter, *J. Chem. Phys.*, 1953, **21**, 836.
65 M. A. Baldo, M. E. Thompson and S. R. Forrest, *Nature*, 2000, **403**, 750.
66 R. J. Holmes, S. R. Forrest, T. Sajoto, A. Tamayo, P. I. Djurovich, M. E. Thompson, J. Brooks, Y.-J. Tung, B. W. D'Andrade, M. S. Weaver, R. C. Kwong and J. J. Brown, *Appl. Phys. Lett.*, 2005, **87**, 243507.
67 B. Park, Y. H. Huh, H. G. Jeon, C. H. Park, T. K. Kang, B. H. Kim and J. Park, *J. Appl. Phys.*, 2010, **108**, 094506.

